Functionalized Micellar Assemblies Prepared via Block Copolymers Synthesized by Living Free Radical Polymerization upon Peptide-Loaded Resins

ARTICLE *in* BIOMACROMOLECULES · JANUARY 2005

Impact Factor: 5.75 · DOI: 10.1021/bm049551y · Source: PubMed

3 AUTHORS, INCLUDING:

David J Liu
Heliosense Biotechnologies Inc.
16 PUBLICATIONS **4,520** CITATIONS
SEE PROFILE

Karen L Wooley
Texas A&M University
328 PUBLICATIONS **17,841** CITATIONS
SEE PROFILE

Functionalized Micellar Assemblies Prepared via Block Copolymers Synthesized by Living Free Radical Polymerization upon Peptide-Loaded Resins

Matthew L. Becker,† Jianquan Liu,‡ and Karen L. Wooley*

Center for Materials Innovation and Department of Chemistry, Washington University, One Brookings Drive, St. Louis, Missouri 63130-4899

Received August 4, 2004; Revised Manuscript Received October 13, 2004

Hybrid peptidic-synthetic amphiphilic block copolymers, synthesized by living free radical polymerization (LFRP) on solid support, have been utilized as precursors for nanoscale materials possessing bio-available peptides. LFRP initiators, coupled to the peptide terminus upon the resin, facilitated the growth of homo- and block copolymers via nitroxide mediated radical polymerization (NMRP) or atom transfer radical polymerization (ATRP). Herein, the versatile solid-support synthesis of the antimicrobial peptide tritrpticin, coupling of living free radical polymerization initiators to the peptide-loaded resin, and the controlled radical polymerization of various monomers to yield amphiphilic diblock copolymers are described. Assembly of the peptidic-synthetic block copolymers into micelles and a preliminary assessment of their in vitro biological properties are detailed.

Introduction

The proliferation of multi-drug resistant bacteria has necessitated the search for new antimicrobial substances and treatment strategies.[1] Antimicrobial peptides and synthetic materials,[2] which are often amphipathic and cationic, are capable of exhibiting bactericidal activity by a mechanism[3] that involves transient pore formation and the disruption of lipid packing.[4] Antimicrobial peptides are typically cationic, a quality which allows them to target the negatively charged cell membranes of bacteria preferentially.[5] Eukaryotic cells have a zwitterionic cell membrane, resulting in a surface that is less attractive to the peptides,[6] and typically requiring high doses, so high that toxicity is a problem for effective in vivo administration.[7] The expanded use of antimicrobial peptides in clinical settings, therefore, will require improvement of their efficacy and/or decreasing their nonselective toxicity. One strategy to enhance the local concentration of functionality involves multi- and polyvalent[8] presentation of bioactive species as a method to combat the bacterial/microbial drug resistance problem. Control of functional group placement, the ability to form charged clusters, and stoichiometry may play crucial roles in the efficacy of the conjugate as well as in tuning effects on cell viability.[9] Recent technological achievements[8,10] have allowed for the synthesis of several mimics of macromolecular assemblies prevalent in nature through the self-assembly of block copolymers. These syntheses afford the creation of well-defined nanostructures possessing surface available functionality.[11−19]

Advances in living polymerizations, including for example cationic,[20] nitroxide mediated radical polymerization[21,22] (NMRP), atom transfer radical polymerization[23] (ATRP), and reversible addition-fragmentation chain transfer (RAFT) polymerization,[24−26] with regard to functional group tolerance and chain-end functionalization,[15,26,27] have afforded the necessary precursors to synthetic nanostructured materials. Previously, the growth of poly(methyl methacrylate) from Wang's solid-phase resin[28] and block copolymers from a protein transduction domain (PTD) derivatized solid-phase resin via NMRP[29] and a peptide sequence from the RGD-containing integrin cell-binding domain of fibronectin, GRGDS, derivatized resin using ATRP[30] were demonstrated. However, virtually any peptide motif and sequence of living radical polymerization conditions can be substituted. These versatile synthetic strategies have demonstrated routes to synthesize peptidic-synthetic block copolymers that are unique in the fact that peptide stoichiometry and regioselectivity of each of the chain segments can be controlled. The procedures extend the realm of polymer materials that can be produced by well-established solid-phase synthesis methods involving both step-growth and chain-growth polymerization mechanisms. In conjunction with our efforts to assemble biologically active micelles and shell cross-linked knedel-like (SCK)[11,31−37] nanoparticles capable of polyvalent interactions with bacteria,[12] DNA,[38] cells,[39−41] or surfaces, NMRP and ATRP methodologies have been employed to facilitate the synthesis of amphiphilic block copolymer precursors that are end-functionalized with the antimicrobial peptide tritrpticin.[42] Herein, efforts to develop general strategies to synthesize peptide derivatized di- and triblock copolymers via NMRP and ATRP on solid support and their assembly into nanostructured materials are described.

* To whom correspondence should be addressed. Tel.: (314) 935-7136. Fax: (314) 935-9844. e-mail: klwooley@artsci.wustl.edu.

† Current Address: National Institute of Standards and Technology, Material Science and Engineering Laboratory, Polymers Division, Gaithersburg, MD 20899-8543.

‡ Current Address: Promega Biosciences, Inc., 277 Granada Dr., San Luis Obispo, CA 94538.

10.1021/bm049551y CCC: $30.25
Published on Web 12/03/2004

Experimental Section

Materials. *tert*-Butyl acrylate (99%), styrene (99%), and toluene (HPLC grade) were purchased from Aldrich Chemical Co. (St. Louis, MO) and purified by stirring over calcium hydride for at least 24 h, followed by distillation under reduced pressure prior to use. Sodium dodecyl sulfate (SDS), 3-(4,5-dimethylthiazol-2-yl)-2,5-diphenyl-2*H*-tetrazolium bromide (98%) (MTT), and Tween20 were purchased from Sigma (St. Louis, MO). Spectra/Por dialysis membranes (Spectrum Laboratories, Inc., Rancho Dominguez, CA) and 96-well polystyrene plates (Falcon) were purchased from Fisher Scientific Company (Pittsburgh, PA). Wang's resin, coupling reagents, and protected amino acids were purchased from Calbiochem-Novabiochem (San Diego, CA). Argon (99.99%) was used in all reactions. All glassware, stir bars, needles, reaction vessels, and syringes were oven dried for at least 24 h, and the glassware was flame-dried under vacuum prior to use.

Measurements. ^{1}H NMR (300 MHz) and ^{13}C NMR (75 MHz) spectra were recorded as solutions on a Varian Mercury 300 MHz spectrometer. ^{1}H NMR (500 MHz) and ^{19}F NMR (470 MHz) spectra were recorded as solutions on a Varian 500 MHz spectrometer with the solvent signal and $CFCl_3$ in as internal and external standards, respectively. IR spectra were obtained on a Perkin-Elmer Spectrum BX FT-IR system. The molecular weights were calculated by ^{1}H NMR spectroscopy. Absorption measurements were made at 405 nm using a Molecular Devices Corp. (Sunnyvale, CA) Thermomax multiplate reader using SOFTmax PRO software. Time-of-flight matrix assisted laser desorption/ionization mass spectrometry (MALDI-TOF) was used to characterize the molecular mass of the peptides and their respective derivatives. Experiments were performed on a PerSeptive Voyager (PerSeptive Biosystems, Framingham, MA) RP-DE MALDI-TOF mass spectrometer with reflectron, delayed-extraction, PSD, and collision-cell capability. Analyses were performed in linear and reflective modes with delayed extraction, DE.

The hydrodynamic diameters and heterogeneity for the micellar constructs in solution (50 mM NaH_2PO_4, 50 mM NaCl, (PBS) pH 7.4) were determined by dynamic light scattering (DLS). The DLS instrumentation was a Brookhaven Instruments Co. (Holtsville, NY) system consisting of a model BI-9000AT digital goniometer, a model EMI-9865 photomultiplier, and a model 95-2 Ar ion laser (Lexel Corp., Palo Alto, CA) operated at 514.5 nm. Measurements were made at 20 ± 1 °C. Prior to analysis, solutions were centrifuged in a model 5414 microfuge (Brinkman Inst. Co., Westbury, NY) for 4 min to remove dust particles. Scattered light was collected at a fixed angle of 90°. The digital correlator was operated with 522 channels, a dual sampling time of 100 ns, a 5 μs ratio channel spacing, and duration of 3 min. A photo multiplier aperture of 200 μm was used, and the incident laser intensity was adjusted to obtain a photon counting of 200 kcps. Only measurements in which the measured and calculated baselines of the intensity autocorrelation function agreed to within 0.1% were used to calculate the particle size. The calculation of the particle size distribution and distribution averages was performed with the ISDA software package (Brookhaven Instruments Co., Holtsville, NY), which employed single-exponential fitting, cumulants analysis, and nonnegatively constrained least-squares particle size distribution analysis routines.

A Beckman Instruments Co. model Optima XL-I analytical ultracentrifuge operated with a model An60-Ti, four-hole rotor was used to centrifuge 50 mM NaH_2PO_4, 50 mM NaCl, (PBS) pH 7.4 solutions of the peptide functionalized micelles to sedimentation equilibrium. All measurements were made at 20 ± 0.1 °C. Rotor speeds of 1500, 2000, and 3000 rpm were used. Sedimentation equilibrium data were obtained for three micelle solution concentrations. Resulting sedimentation equilibrium profiles were recorded with the instrument's Rayleigh interferometric (refractive index) detection optics. The ultracentrifuge sample cell was assembled from an Epon charcoal filled, six channel centerpiece, and matched sapphire windows. The solution volume and the cell's optical path length were 110 μL and 12 mm, respectively. The solution volume and optical path length employed corresponded to a "short" column sedimentation equilibrium experiment with a column height of approximately 2.5 mm. A centrifugation time of 3−5 days was used to reach sedimentation equilibrium. The partial specific volume (ν) for the micelle was determined via sedimentation equilibrium analysis as previously described.[41,43] Density at 20.0 ± 0.1 °C for protonated and deuterated buffers was determined with a Mettler-Parr digital density meter. Measurements of ν were reproducible to within ±1% of the mean value given by three determinations.

Sedimentation velocity data were obtained under identical experimental parameters with the following exceptions. A rotor speed of 25 000 rpm was used. Resulting sedimentation velocity profiles were recorded with the instrument's Rayleigh interferometric (refractive index) detection optics. The ultracentrifuge sample cell was assembled from an Epon charcoal filled, two-channel centerpiece and matched sapphire windows. The solution volume and the cell's optical path length were 400 μL and 12 mm, respectively. The sedimentation time-derivative determines $\partial c/\partial t$ at every radius r by pairwise subtraction of the sedimentation velocity profiles at different times, t. The radius r was then transformed to s^* using

$$s^* = (1/\omega 2t)\ln(r/rm)$$

The $\partial c/\partial t$ are averaged at each s^* to give $g(s^*)$ which represents the mass-weighted distribution of sedimentation coefficients. The sedimentation coefficient, s^*, was corrected to its standard value at 20 °C in water using the following formula, where η_b is corrected buffer viscosity and η_w is the density of water:

$$s_{20,w} = s^*(\eta_b/\eta_w)[(1-\rho\nu)w/(1-\rho\nu)b]$$

where ν and ρ in the term $(1-\rho\nu)w$ correspond to the partial specific volume and the density of water at 20 °C, respectively. The value of s_0 is determined by plotting $s_{20,w}$ versus concentration and extrapolating to zero concentration. By placing the calculated values of d_0, from DLS, and s_0 into

the Svedberg equation shown below, the peak molecular weight, M_p, was calculated

$$M_p = RT\, s_0/d_0\,(1 - \rho\nu)$$

where R is the gas constant, T is the absolute temperature, n is the partial specific volume of the SCK, d_0 is the standardized diffusion coefficient, $d_{20,w}$ is extrapolated to zero concentration, and r is the density of the buffer. The anhydrous sphere diameter, *D0*, of the SCK was then estimated using

$$D_0 = (6M\pi\nu/\pi N_0)^{1/3}$$

Using D_0, and the corrected buffer viscosity, η_b, the frictional coefficient of the anhydrous sphere, f_0, was determined by

$$f_0 = 3p\eta_b D_0$$

The standardized frictional coefficient of the solvated particle, $f_{20,w}$, was calculated using the peak molecular weight, M_p, and the standardized sedimentation coefficient $s_{20,w}$

$$f_{20,w} = M_p(1 - \rho\nu)/s_{20,w}N_0$$

Using the ratio of the standardized frictional coefficient to the value calculated for the anhydrous sphere using the following formula, the maximum degree of hydration, δ_m, was determined

$$\delta_m = \{[(f_{20,w}/f_0)^3 - 1]n\}/0.998234$$

FMOC−Solid-Phase Synthesis of Tritrpticin on Wang's Resin, 1. Tritrpticin (VRRFPWWWPFLRR) was synthesized by standard solid-phase synthesis using FMOC chemistry. For characterization purposes, a small amount (~5 mg) of beads were removed and washed with 1-methyl-2-pyrrolidinone (NMP), *N*,*N*-dimethylformamide (DMF), dichloromethane (CH_2Cl_2), and methanol three times each. Peptide cleavage was achieved through treatment of the resin with 10 mL of a 95% trifluoroacetic acid (TFA)/2.5% triisopropyl silane (TIS)/2.5% water solution for a minimum of 4 h. The solution was filtered with a 0.45 μm filter, and the beads were rinsed with TFA. The solution was concentrated in vacuo and the concentrate was precipitated dropwise into cold ether. The precipitates were centrifuged at 3500 rpm for 10 min. The supernatant was decanted, the pellet was resuspended in cold ether, and the centrifugation process was repeated. The pellet was dried, dissolved into water, and purified by reversed phase HPLC. IR: 3339 (br), 2958, 2868, 1695, 1532, 1443, 1212, 1135, 836, 800. λ_{max} = 280 nm. MS: $C_{96}H_{132}N_{28}O_{14}$ (MALDI): 1902.99 $[M+1]^+$ (calc: 1901.0 MW).

Derivatization of Tritrpticin with a Glutaric Anhydride Linker, 2. The Tritrpticin loaded resin (1.00 g, 0.90 mmol/g) was washed with NMP, methanol, and CH_2Cl_2 each three times. Glutaric anhydride (508.0 mg, 4.5×10^{-3} mol) was dissolved in DMF (5.00 mL) and transferred to the SPS vessel. The mixture was agitated via bubbling with nitrogen for 24 h. A negative Kaiser test indicated that no free amine groups remained. Cleavage and purification methods were identical to those described previously. IR: 3339 (br), 3200, 2958, 2869, 1695, 1690, 1600, 1550, 1535, 1450, 1202, 1135, 836, 800, 730, 721. λ_{max} = 280 nm. MS: $C_{101}H_{138}N_{28}O_{17}$ (MALDI): 2107.20 $[M+H]^+$ (calc: 2106.0 MW).

Coupling of *N*-*tert*-Butyl-*O*-[1-(4-aminomethylphenyl)-ethyl]-*N*-(2-methyl-1-(4-fluorophenyl)propyl)hydroxylamine to the Linker Derivatized Resin, 4. The tritrpticin loaded, linker derivatized resin **2** (905.1 mg, 0.90 mmol/ g) was washed with NMP, MeOH, and CH_2Cl_2 each three times. *N*-*tert*-Butyl-*O*-[1-(4-aminomethylphenyl)ethyl]-*N*-(2-methyl-1-(4-fluorophenyl)propyl) hydroxylamine, **3** (1.4000 g, 4.1 $\times 10^{-3}$ mol), HOBt (1.2006 g, 7.8×10^{-3} mol), and DIC (1.22 mL, 7.8×10^{-3} mol) were dissolved in *N*,*N*-dimethyl formamide (5.00 mL) and transferred to the SPS vessel. The mixture was agitated via bubbling with nitrogen for 24 h. A negative Kaiser test indicated that no free amine groups remained. Peptide cleavage and purification was identical to methods described previously. MS (MALDI): 2370.4582 $[M+H]^+$ (calc: 2369.3 MW).

NMRP-based Preparation of Tritrpticin-*b*-poly(*tert*-butyl acrylate), 5, and Cleavage from the Resin to Afford 8. A 100 mL Schlenk flask that had been oven dried overnight, flame dried under vacuum, and back filled with argon was charged with dry resin beads, **4** (500.0 mg, 0.9 mmol/g), loaded with the fluorinated alkoxyamine coupled to the linker derivatized tritrpticin. *Tert*-butyl acrylate (20.00 mL, 1.36×10^{-3} mol) and 2,2,5-trimethyl-4-(4′-fluorophenyl)-3-azahexane-3-oxyl, **7** (15.0 mg, 6.3×10^{-5} mol) were added via an argon washed syringe. The solution was degassed by three cycles of freeze−pump−thaw, and following the final thaw cycle, the mixture was allowed to stir for 10 min before being immersed in an oil bath at 135 °C. After 8 h, the oil bath was removed and the reaction vessel was immersed in liquid nitrogen to quench the polymerization reaction. The solution was filtered, washed with THF, and rinsed 3 times each with DMF, CH_2Cl_2, and MeOH. A small amount of beads were cleaved, and the product was precipitated and purified by dialysis against water (MWCO 1000 Da) yielding tritrpticin-*b*-poly(acrylic $acid_{185}$) **8**. The pellet was dried, dissolved into water, and purified by extensive dialysis (1000 MWCO) against water for 48 h. T_g = 133 °C. IR: 3400, 2950, 1795, 1700, 1650, 1540, 1440, 1200, 1130, 835, 795, 700 cm^{-1}. Tritrpticin-poly(acrylic $acid_{185}$) M_n: (^{1}H NMR: 13,200 Da) as calculated from ^{1}H NMR end group analysis.

NMRP-based Preparation of Tritrpticin-*b*-poly(*tert*-butyl acrylate)-*b*-polystyrene (6) and Cleavage from the Resin to Afford 9. A 100 mL Schlenk flask that was prepared in the usual manner was charged with dry resin beads, **5** (400.0 mg, 0.90 mmol/g), loaded with the poly(*tert*-butyl acrylate) macroinitiator coupled to the solid support. Styrene (20.00 mL, 1.74×10^{-3} mol) and 2,2,5-trimethyl-4-(4′-fluorophenyl)-3-azahexane-3-oxyl, **7** (15.0 mg, 6.3×10^{-5} mol) were added via argon washed syringe. The solution was degassed as described previously before being immersed in an oil bath at 135 °C. After 8 h, the polymerization was quenched in liquid nitrogen and washed with THF. Approximately half of the beads were subjected to cleavage conditions, and the product was precipitated and purified by dialysis against water (MWCO 1000 Da) yielding

9. Following lyophilization, the isolated product amounted to approximately 45 mg. $(T_g)_1 = 131$ °C. $(T_g)_2 = 99$ °C. IR: 3400, 2920, 1941, 1870, 1750, 1700, 1650, 1500, 1440, 1300, 1140, 1135, 914, 700 cm^{-1}. Tritrpticin-poly(acrylic $acid_{185}$-*b*-$styrene_{24}$) M_n: (^{1}H NMR: 18,100 Da) as calculated from ^{1}H NMR end group analysis.

Coupling of 2-Bromo-isobutyryl bromide to the Tritrpticin-loaded Resin, 10. A total of 1.0002 g (0.90 mmol/ g) of dried tritripticin loaded resin beads was transferred to the solid-phase synthesis vessel. The resin was soaked with triethylamine (5.00 mL, 3.64×10^{-2} mol), and 2-bromo isobutyryl bromide (3.00 mL, 2.43×10^{-2} mol) was added. The mixture was then shaken at ambient temperature for 4 h. The solution was filtered and washed with DMF, MeOH, and CH_2Cl_2 three times each. The resulting yellow resin was ready for atom transfer radical polymerization on solid support. A small amount of beads were cleaved, precipitated, and purified by reverse phase HPLC. IR: 2920, 1750, 1440, 1270, 1130, 850 cm^{-1}. MS (MALDI): $[M+H]^+$ 2052.6635 (calculated: 2051.24).

ATRP-based Preparation of Tritrpticin-*b*-poly(*tert*-butyl acrylate), 11, and Cleavage from the Resin to Afford 13. A 100 mL Schlenk flask with ground glass sidearm was attached to a double manifold and fitted with a condenser. The atmosphere was removed, and the assembly was flame-dried under vacuum and back-filled with argon. The dried ATRP initiator loaded on the solid-phase resin beads (278.2 mg, 2.5×10^{-4} mol) were added to the cooled Schlenk flask. The resin was pumped under vacuum for an hour to remove all residual solvent. Copper (I) bromide (255.2 mg, 1.8×10^{-3} mol) was measured under inert atmosphere in a glovebag and added to the reaction vessel. The assembly was then evacuated and back-filled twice to minimize oxygen contamination. The monomer was deoxygenated, via bubbling with argon, prior to addition. The monomer (3.50 mL, 1.8×10^{-3} mol) and PMDETA (370 μL, 1.8×10^{-3} mol) were added sequentially via an argon-washed syringe. A degassing cycle of freeze−pump−thaw followed each addition. The reaction was allowed to stir for 10 min prior to the vessel being immersed in a 70 °C oil bath for 4 h. After the desired reaction time, the polymerization was quenched in liquid nitrogen and washed with THF. A small amount of beads were cleaved, and the product was precipitated and purified by dialysis against water (MWCO 1000 Da) yielding tritrpticin-*b*-poly(acrylic $acid_{42}$), **13**. $(T_g)_1$: 137 °C. IR: 3400, 2920, 1750, 1550, 1130 cm^{-1}. Tritrpticin-poly(acrylic $acid_{42}$) M_n: (^{1}H NMR: 4,900 Da) as calculated from ^{1}H NMR end group analysis.

ATRP-based Preparation of Tritrpticin-*b*-poly(acrylic acid-*b*-styrene), 12, and Cleavage from the Resin to Afford 14. A 100 mL Schlenk flask with ground glass sidearm was attached to a double manifold and fitted with a condenser. The atmosphere was removed, and the assembly was flame-dried under vacuum and back-filled with argon. The dried homopolymer loaded on the solid-phase resin beads (778.0 mg, 7.0×10^{-4} mol) was added to a cooled Schlenk flask. Copper (I) bromide (370.4 mg, 2.6×10^{-3} mol) was measured under inert atmosphere in a glovebag and added to the reaction vessel. The assembly was then evacuated and back-filled twice to minimize oxygen contamination. The monomer was deoxygenated, via bubbling with argon, prior to addition. The monomer (10.00 mL, 8.73 $\times 10^{-2}$ mol) and PMDETA (586 μL, 2.8×10^{-3} mol) were added sequentially via an argon-washed syringe. A degassing cycle of freeze−pump−thaw followed each addition. The reaction was allowed to stir for 10 minutes prior to the vessel being immersed in a 70 °C oil bath for 6 h. After the desired reaction time, the polymerization was quenched in liquid nitrogen and washed with THF. A small amount of beads were cleaved, and the product was precipitated and purified by dialysis against water (MWCO 1000 Da) yielding tritrpticin-*b*-poly(acrylic $acid_{42}$-*b*-$styrene_{11}$), **14**. $(T_g)_1$: 135 °C. $(T_g)_2$: 103 °C. IR: 3070, 3050, 2920, 2800, 1940, 1870, 1800, 1595, 1500, 1535, 1270 cm^{-1}. Tritrpticin-poly(acrylic $acid_{42}$-*b*-$styrene_{11}$) M_n: (^{1}H NMR: 6,100 Da) as calculated from ^{1}H NMR end group analysis.

Micelle Formation (13). Spherical micelles of narrow size distribution were obtained by dissolving the purified block copolymer **9** (20.0 mg, 1.10×10^{-6} mol) in THF, followed by gradual addition (10.0 mL/h) of an equal volume of nonsolvent (H_2O) for the hydrophobic polystyrene to induce micelle formation. A cloudy texture developed when 15−20 vol % water was added indicating the formation of micelles. The micelles were allowed to stir overnight before being transferred to a presoaked and rinsed dialysis bag (MWCO 12 000−14 000 Da) and dialyzed against deionized water for 3 days to remove the remaining organic solvent. The hydrodynamic diameters (D_h) of the micelles in Nanopure water (17.3 mΩ-cm) were determined by dynamic light scattering. $D_h = 51 \pm 5$ nm, $S_{20,w} = 38.0$, $\nu = 0.658 \pm 0.011$ mL/g, $M_p = 2.692 \times 10^6$ Da, $N_{agg} = 149 \pm 10$, $D_0 = 23.6$ nm, $d_{20,w} = 1.01 \times 10^{-7}$ g/mL, $d_0 = 9.98 \times 10^{-8}$ g/mL, $f_{20,w}/f_0 = 1.70$, $\delta_m = 2.63$ g_{H2O}/g_{SCK}.

Minimum Inhibitory Concentrations (MIC). The MIC of the controls and derivatized micelles were determined by standard microtiter broth dilution methods against Gram-negative (*Echerichia coli*, Stratagene XL-1 Blue) and Gram-positive (*Staphyloccus aureus*, ATCC 6538P) bacteria. Briefly, single colonies of bacteria were inoculated into their respective culture mediums (SAMS media, *S. aureus*) and LB, *E. coli*) and incubated overnight at 37 °C. An aliquot of the culture was transferred to a Erlenmeyer flask with 200.0 mL of fresh culture media and incubated at 37 °C until mid-logarithmic growth (OD $\lambda_{600} = 0.50$) was obtained for each organism. A 2-fold dilution series was prepared for each sample to be tested. All of the substances to be tested were taken up in the respective culture media. The concentrations of the solutions were 1000 mg/L, and 150 μL was placed in each row of the first two columns and diluted accordingly. A total of 150 μL of the mid-log phase growth *S. aureus* and *E. coli* was then added to each well in columns 1−11 in 96-well plates. Column 12 was inoculated with fresh, sterile media. The plates were incubated for 12 h at 37 °C and their OD's (abs. = λ_{600}) were measured in a 96-well plate reader. The reported values are the results of quadruplicate measurements from two independent assays. MIC was defined as the point at which no bacterial growth was seen relative to controls.

Cell Viability Assay. Mouse myeloma B cells, ATCC (Manassas, VA) CRL-1581.1, were cultured in Roswell Park Memorial Institute (RPMI) 1640 media using TCM serum replacement obtained from Celox Laboratories (St. Paul, MN) and maintained at 37 °C in a humidified atmosphere of 5% CO_2. Cell viability was determined by enzymatic MTT assay. Briefly, mouse myeloma B cells were diluted into fresh media at concentrations of 50 000 cells/mL, and 100 μL was added to each well in a 96-well plate. A separate 96-well plate was used for each polymer and SCK sample. After cell seeding, the plates were placed in an incubator (37 °C, 5% CO_2) and allowed to grow for 24 h. Fresh 96-well plates were loaded with 40 μL of sterile buffer, and the first column of each row was loaded with polymer or SCK stock solutions of known concentration and then serially diluted with the last column held as a control with no polymer or micelle added. A total of 50 μL of fresh media was then added to every well in the serially diluted plates. The original plates were removed from the incubator and checked for bacterial contamination, and the premixed sample solutions were transferred to the seeded plates, which were then returned to the incubator. After 24 h, 20 μL of MTT (5.00 mg/mL) in PBS (50 mM phosphate, 50 mM sodium chloride, pH 7.4,) was added to each well. The plates were returned to the incubator and allowed to equilibrate for 2 h. After 2 h, 80 μL of extraction buffer (20% w/v sodium dodecyl sulfate (SDS, Sigma) in 50:50 DMF: H_2O, pH 4.7) was added to each well to extract the aqueous insoluble formazan product. The plates were then incubated for 18 h to allow for the formazan extraction after which the absorbance of each solution was measured at 560 nm. Concentrations were determined by the mass of lyophilized polymer sample dissolved in PBS and then adjusted for the dilution of the media. Results are an average of four values and the standard deviation is reported for each concentration.

Results and Discussion

Tritrpticin is a peptide having a sequence of 13 amino acid residues that has demonstrated strong antimicrobial activity against a variety of pathogens.[44] It is a member of the cathelicidin class of antimicrobial peptides which are synthesized in myeloid cells[45] and are expressed as preproteins. As seen in Scheme 1, the 100+ amino acid residue "pro" region of the protein is a conserved sequence within this family of cathelicidin peptides. The shorter "pre" sequence directs the protein for secretion, and the antimicrobial domain, which precedes the "pro" sequence, is carried along in an inactive state until it is clipped from the protein by elastase-like protease.[46] Although the exact mode of action is unknown, the amphipathic structure of tritrpticin is reported to perturb cellular membranes. Fluorescence studies have indicated that the peptide locates to varying degrees at the water−lipid interface of surfactant micelles. The continued antimicrobial effects and time-dependent quenching experiments described elsewhere[42,47,48] suggest that the peptide embeds itself in the lipid bilayer. These were essential findings to the strategy described herein, which exploits the polyvalent surface interactions enabled by incorporation of the peptide into nanoscale block copolymer micelles. The wide scope of activity exhibited by tritrpticin provides a bioactive species that can be incorporated into the exploratory conjugation of different linkers, LFRP initiators, and block copolymers as precursors for nanostructured materials. Tritrpticin is the only known natural sequence to possess three consecutive tryptophan residues,[44] (Scheme 1) and the three aromatic residues provide an additional tool when characterizing the initiators and determining the molecular weights of the polymeric precursors.

Scheme 1. Tritrpticin (VRRFPWWWPFLRR) Peptide Shown as the Variable Domain at the End of the Pre-pro Peptide Domains Which Are Largely Conserved within the Cathelicidin Family of Antimicrobial Peptides[a]

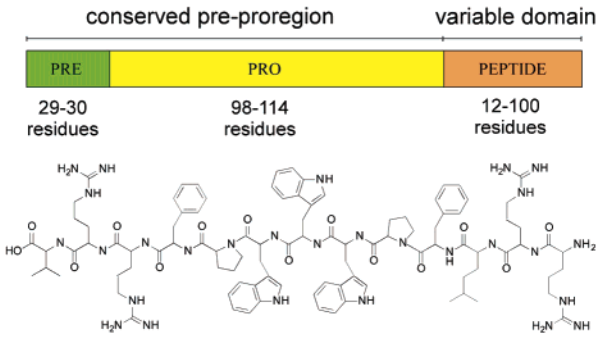

[a] The distinct fold in the 3D structure of this peptide and the separation of the cationic residues from the hydrophobic residues result in an amphipathic structure, which is believed to be the structural feature that leads to antimicrobial activity.

The peptidic block copolymers were assembled upon solid support as depicted in Scheme 2. Tritrpticin was assembled on Wang's resin via FMOC solid-phase strategies. The N-terminus of this peptide sequence **1** was converted to a carboxy functional group **2** by coupling with glutaric anhydride which also functioned as a short linker. Further derivitization by functionalizing the carboxy end group of **2** with the benzylamine group on the fluorine-labeled alkoxyamine **3** yielded an NMRP initiator tethered to the N-terminus of the bio-active peptide **4**, all of which was bound to a solid support. The fluorinated nitroxide and alkoxyamine derivatives were prepared by methods according to those described by Hawker.[49,50] Small portions of **1**, **2**, and **4** were cleaved at their respective stages of the synthesis, and their purities were confirmed by mass spectrometry. The presence of four diastereomers in the alkoxyamine initiator[50] provided for rapid identification of the respective peaks in the NMR spectra of the derivatized peptide. The diastereomers were the result of coupling via Jacobsen's catalyst and were assigned easily when the initiator was attached to the peptide species, as shown in Scheme 2. The resonances in the ^1H and ^{19}F NMR spectra of the respective diastereomers of the initiator **3**, visualized in Figure 1, were observed at the same locations when coupled to the peptide, **4**. Additional evidence for efficient coupling of the peptide to the linker and the initiating species was provided by mass spectrometry. Furthermore, the presence of a fluorine atom at the end of each peptidic-synthetic polymer chain provided a unique characterization handle that was observed by infrared spectroscopy and solution and solid-state ^{19}F NMR spectroscopies.

Scheme 2. Synthetic Strategy for the Synthesis of Peptidic-Synthetic Block Copolymer Precursors to Nanostructured Materials from Tritrpticin-Loaded Solid Support via Nitroxide Mediated Radical Polymerization

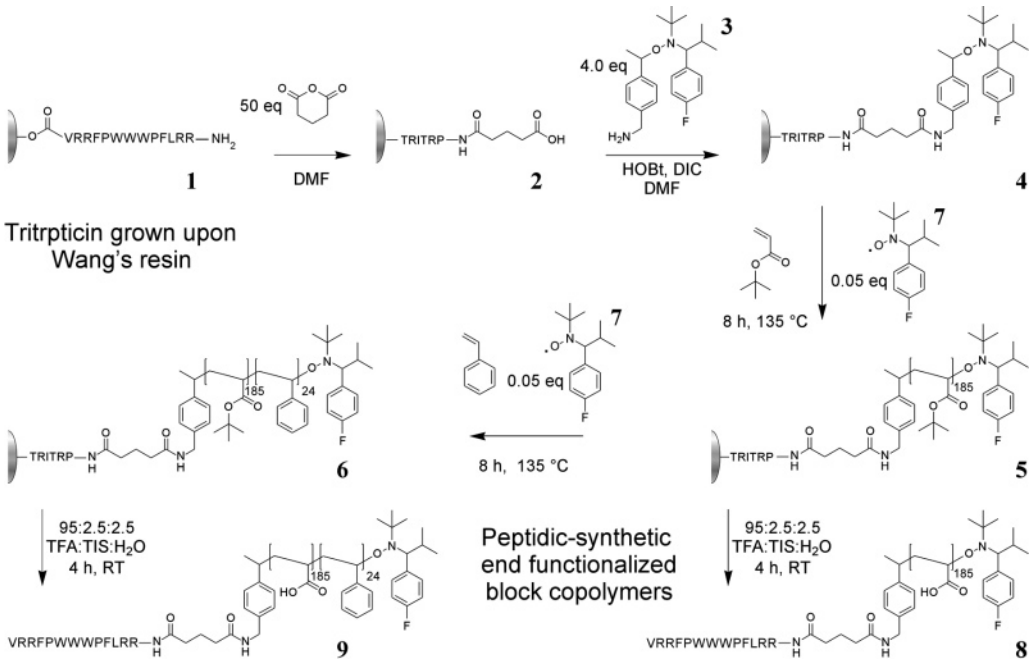

The supported NMRP initiator was then used to perform chain polymerization from the terminus of the initial step-growth peptidic macroinitiators and create block copolymers. The NMRP was conducted by charging a 100 mL Schlenk flask with dry resin beads **4**, *tert*-butyl acrylate, and 0.05 molar excess of 2,2,5-trimethyl-4-(4′-fluorophenyl)-3-azahexane-3-oxyl, **7**, degassing by three cycles of freeze−pump−thaw, and following the final thaw cycle, immersing the mixture in a preheated oil bath, and allowing polymerization to occur at 135 °C for 8 h. Cleavage of the bio-conjugate was described previously,[29] and this procedure facilitated the removal of side-chain protecting groups as well as cleavage of the *tert*-butyl esters of the poly(*tert*-butyl acrylate) segment, to yield the diblock copolymer, **8**. Following purification, **8** was determined to have approximately 185 acrylic acid repeat units as calculated from ^{1}H NMR spectroscopy.

The chain was further extended with a hydrophobic block segment, via initiation of styrene polymerization from the NMRP initiator that remained present at the terminus of the poly(*tert*-butyl acrylate) segment. Styrene and an additional 0.05 molar excess of 2,2,5-trimethyl-4-(4′-fluorophenyl)-3-azahexane-3-oxyl, **7**, were added to dry peptide-poly(*tert*-butyl acrylate) macroinitiator-loaded resin beads, **5**, and then allowed to undergo polymerization while being heated in an 135 °C oil bath for 8 h. Cleavage and purification yielded a peptidic-synthetic triblock copolymer, **9**, with approximately 24 styrene repeat units, as measured by ^{1}H NMR spectroscopy. The resulting molecular weight of the triblock copolymer upon removal of the protecting groups and *tert*-butyl esters was approximately 18 100 Da. The small degree of styrene incorporation suggests that a portion of the reactive chain ends was lost in the first polymerization or during the workup procedures. An alternative explanation is that the polymerization efficiency was low due to solvent incompatibilities and the poor solubility of brushes growing from the solid support resin in styrene. The presence of growing polymeric species was confirmed by MALDI mass spectrometry. The block copolymer exhibited glass transitions at 131 and 99 °C, indicative of the acrylic acid and styrene block segments, as observed by differential scanning calorimetry.

Atom Transfer Radical Polymerization. To further demonstrate the versatility of the solid-phase synthetic approach, ATRP methodologies were employed. In this case, the solid-phase resin beads loaded with the tritrpticin peptide, **1**, were derivatized with 2-bromo isobutyryl bromide to afford **10** as shown in Scheme 3. A small amount of functionalized beads were allowed to undergo cleavage, and the ATRP-initiator-functionalized peptide was confirmed by ^{1}H NMR spectroscopy and mass spectrometry. As shown in Figure 2, the methyl groups alpha to the carbonyl of the initiator can be readily identified in the enlarged region of the ^{1}H NMR spectra.

The ATRP of *tert*-butyl acrylate was allowed to proceed from the initiator-derivatized peptide on support, **10**, at 70 °C for 4 h. Cleavage and purification of **11** afforded tritrpticin-*b*-poly(acrylic acid), **13**. Molecular weight characterization by ^{1}H NMR end-group analysis determined the addition of approximately 42 acrylic acid repeat units. Formation of the amphiphilic triblock was accomplished by the subsequent ATRP of styrene at 70 °C for 6 h from the tritrpticin-*b*-poly(*tert*-butyl acrylate), **11**, chain-end affording **12**, which when cleaved from the resin yielded **14**. Tritrpticin-*b*-poly(acrylic acid-*b*-styrene) was found to have incorporated approximately 11 styrene repeat units by ^{1}H NMR end group analysis. The resulting molecular weight of the triblock copolymer upon removal of the peptide protecting groups and *tert*-butyl esters was approximately 6100 Da. The presence of polymeric material was confirmed by MALDI-TOF mass spectrometry and differential scanning calorimetry (DSC). The block copolymer exhibited glass transitions at

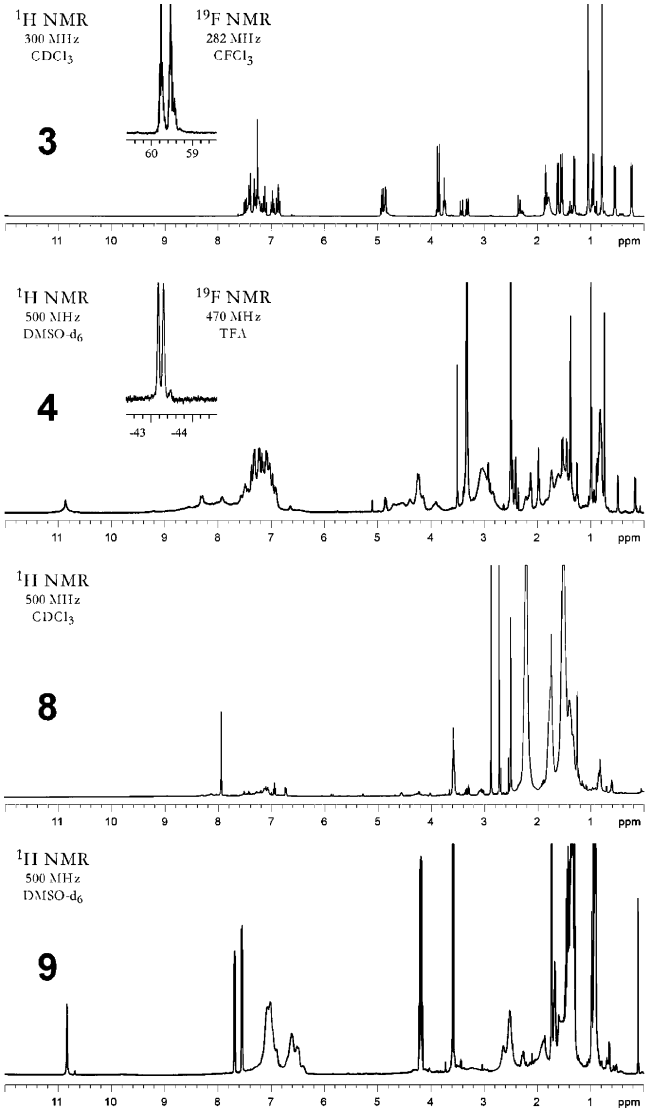

Figure 1. ^{1}H and ^{19}F NMR spectra of ^{19}F-labeled NMRP alkoxyamine initiator, **3**, tritrpticin conjugated ^{19}F-labeled NMRP alkoxyamine initiator, **4**, tritrpticin-*b*-PAA_{185}, **8**, and tritrpticin-*b*-PAA_{185}-*b*-PS_{24}, **9**.

135 and 103 °C, indicative of the acrylic acid and styrene block segments, as observed by differential scanning calorimetry. Due to the limited solubility and compatibility of the amphiphilic peptidic-synthetic block copolymers with available size exclusion chromatography methods, the polymers were not analyzed by size exclusion chromatography.

Micelles of narrow size distribution were obtained by dissolving the respective block copolymer in THF (20.0 mg, 1.0 mg/mL), followed by gradual addition of H_2O (20.00 mL, 10 mL/min) to induce micelle formation as depicted in Figure 3. The number average NNLS fit of dynamic light scattering data, Figure 4, shows that the majority of the particles are 51 nm in size. Micelles of this size are fairly consistent with block copolymer micelles seen previously.[51,52] The small fraction of larger material detected is presumed to result from larger-scale aggregates.

The size, shape, and hydration of the micelles were determined using a combination of sedimentation equilibrium (SE) and sedimentation velocity (SV) analytical ultracentrifugation experiments. The experimentally determined parameters of the micelle were determined using methods

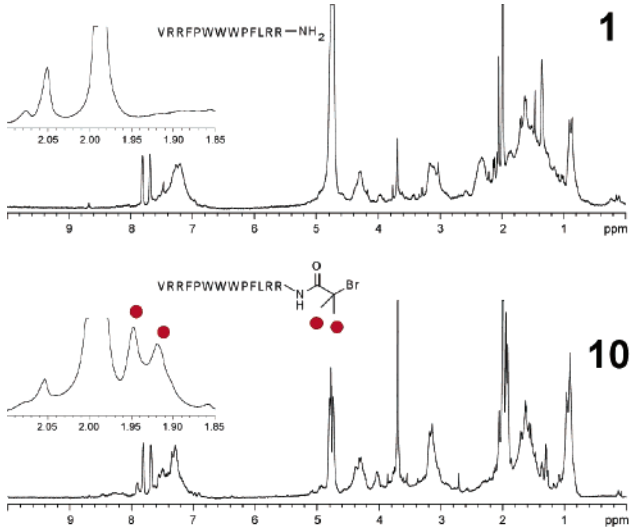

Figure 2. ^{1}H NMR (500 MHz, DMSO-d_6) spectra of tritrpticin, **1**, and tritrpticin derivatized with 2-bromoisobutyryl bromide, **10**, which was then used to initiate atom transfer radical polymerization from the peptide loaded solid-support. The methyl groups are readily identifiable at 1.91 and 1.95 ppm in the enlarged ^{1}H NMR.

Scheme 3. Synthetic Strategy for the Synthesis of Peptidic-Synthetic Block Copolymer Precursors to Nanostructured Materials from Tritrpticin Loaded Solid Support via Atom Transfer Radical Polymerization

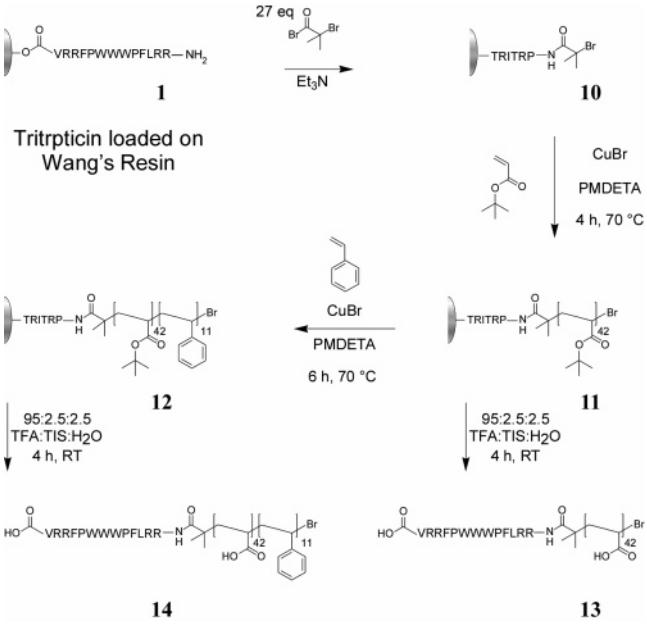

described previously.[36,43] After determining the partial specific volume using SE, a SV experiment was performed to determine several additional parameters. The distribution of mass of the micelle is represented by the generation of a sedimentation coefficient distribution from the time-averaged derivative ($g(s^*)$) of the sedimentation velocity boundaries. The monomodal distribution represents the most probable value of the sedimentation coefficient, s^*, which was measured to be 35.8. The derivable parameters were corrected to their standard values at 20 °C in water. The coefficients were used to derive the peak molecular weight, M_p, using the Svedberg equation. The aggregation number, N_{agg}, or number of chains per micelle can be approximated by the ratio of the peak molecular weight, M_p, of the particle

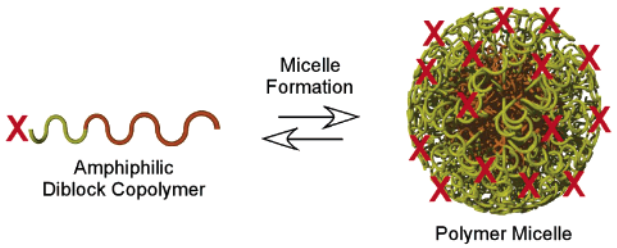

Figure 3. Poly(acrylic acid-*b*-styrene) block copolymer precursor end-functionalized with tritrpticin affords well-defined micelles when dissolved in a good solvent for all portions of the precursor and a poor solvent for the hydrophobic polystyrene is added.

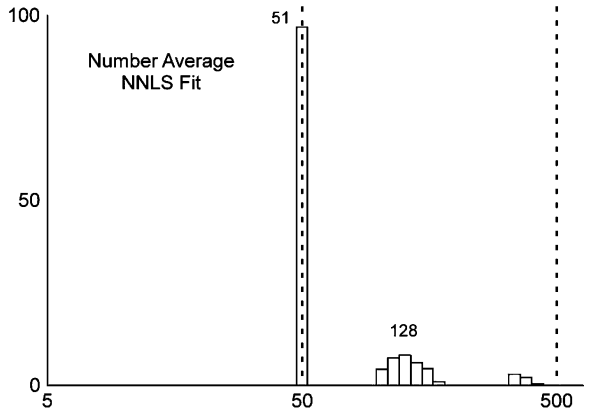

Figure 4. Number average NNLS fit shows that the majority of the particles are 51 ± 5 nm in size. The small fraction of larger material detected is presumed to be higher order aggregates.

to the molecular weight of the amphiphilic block copolymer precursor, 18 100 Da. Using the molecular weight of the micelle, **13**, 2.692 × 10^6 Da, the aggregation number, N_{agg}, was found to be 149 ± 10. This corresponds to approximately 149 ± 10 tritrpticin peptides per micelle. The diameter of the anhydrous sphere, D_0, was calculated to be 23.6 nm. The degree of hydration, d_m, in the micelle as measured in the sedimentation velocity experiment was found to be 2.62 g H_2O/g micelle.

Biological Properties. The antimicrobial activities of tritrpticin and the micellar construct were assessed against *Staphylococcus aureus* and *Echerichia coli* by broth microdilution assay to determine the minimum inhibitory concentration (MIC). Tritrpticin has been shown to be effective against *S. aureus* and *E. coli* at 16 and 32 μg/mL, respectively.[48] Comparative assays were performed to assess the antimicrobial properties of both the peptide and the peptide functionalized micelle. As seen below in Figure 5, tritrpticin was effective against *S. aureus* at 17 μg/mL and *E. coli* at 33 μg/mL. The micelles, which are composed of approximately 10% by mass tritrpticin, as calculated from the experimentally determined micelle mass, aggregation number, and block copolymer mass, were effective against *S. aureus* and *E. coli* at 13 and 13 μg/mL, respectively.

Tritrpticin has also demonstrated strong (unfavorable) hemolytic properties against human red blood cells (hRBC) in vitro. The hemolytic effects were approximately 37% at 100 μg/mL (52 μM).[48] These cytotoxic effects are of concern when considering the further use of tritrpticin and tritrpticin decorated nanostructures in vivo. The cell viability in the presence of the polymeric constructs was evaluated by MTT

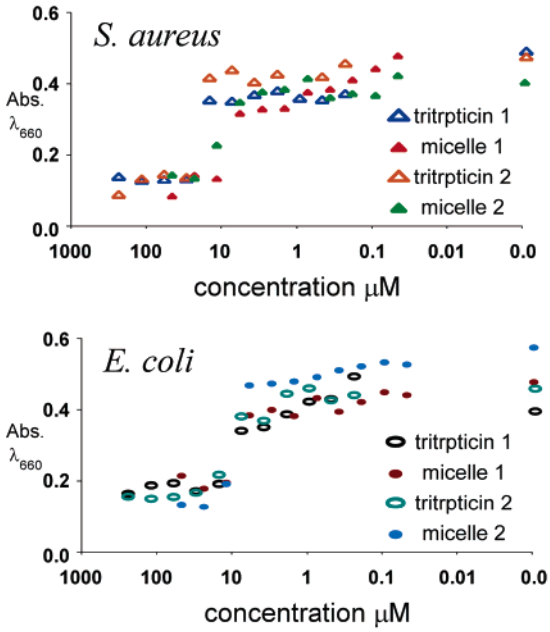

Figure 5. Derivatized micelles (closed symbols) consisting of tritrpticin end-functionalized amphiphilic block copolymers showed lower MIC's against both *S. aureus* (triangles) and *E. coli* (circles) than the tritrpticin peptide itself (open symbols). Numbers 1 and 2 represent identical experiments run on different days.

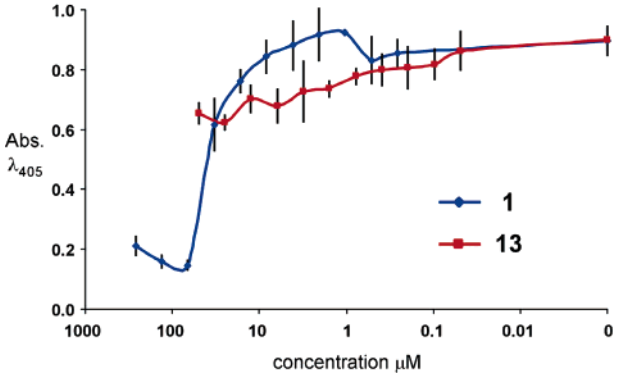

Figure 6. Assembly of amphiphilic block copolymers end-functionalized with tritrpticin into micelles reduced the detrimental effects of the constructs on cell viability. The tritrpticin derivatized constructs were not detrimental to the viability of the cells at 50 μM, whereas the peptide was toxic to the cells at 33 μM.

assay.[40,53] As demonstrated previously, micelles[54] and SCKs[40] possessing poly(acrylic acid) shells do not affect significantly the viability cells. In Figure 6, tritrpticin was shown to be toxic to the mouse myeloma B cells at approximately 33 μM concentrations. The tritrpticin functionalized micelles, **13**, did not affect the viability of the cells at concentrations up to 50 μM, tritrpticin equivalence, the highest concentration evaluated.

Conclusions

The syntheses of tritrpticin derivatized amphiphilic block copolymers on solid support have been described. Block copolymer growth from the living free radical polymerization initiator loaded resins via NMRP and ATRP has been detailed. Incorporation of the peptide into micellar constructs demonstrated enhanced anti-microbial activity relative to the free peptide while appearing to temper the detrimental effects

on cell viability in vitro. The data presented herein further demonstrate that at least a fraction of the peptide motif is both bioavailable and bioactive when conjugated to the nanostructure. Extension of this technology holds promise for the attachment of ligands, small molecule drugs, and linkers in a combinatorial fashion to create a new library of amphiphilic polymer building blocks applicable to nanotechnology and biomedicine. In addition, without self-assembly into micelles, peptidic block copolymers may also serve as stand-alone drugs with increased molecular weight and fine-tuned pharmacokinetic properties.

Acknowledgment. This material is based upon work supported by the National Science Foundation under Grant Numbers DMR-9974457 and 0210247. A fellowship from the Department of Education Government Assistance for Areas of National Need (GAANN) Program (P200A80221), and a Training Fellowship for the Chemistry-Biology Interface Program at Washington University funded by the NIH-NRSA (5-T32-GM08785-02) are also gratefully acknowledged. Assistance from André d'Avignon from the Washington University High Resolution NMR facility in the collection and interpretation of high field ^{1}H and ^{19}F NMR spectra is greatly appreciated. The authors also thank Mr. Jeffrey L. Turner for production of the schematic SCK illustrations.

References and Notes

(1) Lohner, K. *Development of novel antimicrobial agents: emerging strategies*; Horizon Scientific Press: Norfolk, U.K., 2001.
(2) (a) Patel, M. V.; Patel, S. A.; Ray, A.; Patel, R. M. *J. Polym. Sci., Part A: Polym. Chem.* **2004**, *42*, 5227−5234. (b) Arnt, L.; Nüsslein, K.; Tew, G. N. *J. Polym. Sci., Part A: Polym. Chem.* **2004**, *42*, 3860−3864. (c) Braun, M.; Sun, Y. *J. Polym. Sci., Part A: Polym. Chem.* **2004**, *42*, 3818−3827. (d) Sauvet, G.; Fortuniak, W.; Kazmierski, K.; Chojnowski, J. *J. Polym. Sci., Part A: Polym. Chem.* **2004**, *42*, 2939−2948. (e) Patel, S. A.; Patel, M. V.; Ray, A.; Patel, R. M. *J. Polym. Sci., Part A: Polym. Chem.* **2003**, *41*, 2335−2344. (f) Bozja, J.; Sherrill, J.; Michielsen, S.; Stojilijkovic, I. *J. Polym. Sci., Part A: Polym. Chem.* **2003**, *41*, 2297−2303. (g) Lee, S. B.; Koeopsel, R.; Stolz, D. B.; Warriner, H. E.; Russell, A. J. *J. Am. Chem. Soc.* **2004**, *ASAP article*; DOI 10.1021/ja048463i.
(3) Epand, R. M.; Vogel, H. J. *Biochim. Biophys. Acta* **1999**, *1462*, 11−28.
(4) (a) Giangaspero, A.; Sandri, L.; Tossi, A. *Eur. J. Biochem.* **2001**, *268*, 5589−5600. (b) Shai, Y. *Biopolymers* **2002**, *66*, 236−248.
(5) Zasloff, M. *Nature* **2002**, *415*, 389−395.
(6) Chu-Kung, A. F.; Bozzelli, K. N.; Lockwood, N. A.; Haseman, J. R.; Mayo, K. H.; Tirrell, M. V. *Bioconjugate Chem.* **2004**, *15*, 530−535.
(7) Darveau, R. P.; Cunningham, M. D.; Seachord, C. L.; Cassianoclough, L.; Cosand, W. L.; Blake, J.; Watkins, C. S. *Antimicrob. Agents Chemother.* **1991**, *35*, 1153−1159.
(8) Mammen, M.; Choi, S. K.; Whitesides, G. M. *Angew. Chem., Int. Ed.* **1998**, *37*, 2754−2794.
(9) Tam, J. P.; Lu, Y.-A.; Yang, J.-l. *Eur. J. Biochem.* **2002**, *269*, 923−932.
(10) Niemeyer, C. H. *Angew. Chem., Int. Ed.* **2001**, *40*, 4128−58.
(11) Qi, K.; Ma, Q.; Remsen, E. E.; Clark, C. G., Jr.; Wooley, K. L. *J. Am. Chem. Soc.* **2004**, *126*, 6599−6607.
(12) Joralemon, M. J.; Murthy, K. S.; Remsen, E. E.; Becker, M. L.; Wooley, K. L. *Biomacromolecules* **2004**, *5*, 903−913.
(13) Accardo, A. T., D.; Roscigno, P.; Gianolio, E.; Paduano, L.; D'Errico, G.; Pedone, C.; Morelli, G. *J. Am. Chem. Soc.* **2004**, *126* (10), 3097−3107.
(14) Pakstis, L. M.; Ozbas, B.; Hales, K. D.; Nowak, A. P.; Deming, T. J.; Pochan, D. *Biomacromolecules* **2004**, *5*, 312−318.
(15) Orfanou, K.; Topouza, D.; Sakellariou, G.; Pispas, S. *J. Polym. Sci. Part A: Polym. Chem.* **2003**, *41*, 2454−2461.
(16) Power-Billard, K. N.; Spontak, R. J.; Manners, I. *Angew. Chem., Int. Ed.* **2004**, *43*, 1260−1264.
(17) Hernández, J. R.; Klok, H.-A. *J. Polym. Sci. Part A: Polym. Chem.* **2003**, *41*, 1167−1187.
(18) Klok, H.-A. *Angew. Chem., Int. Ed.* **2002**, *41*, 1509−1513.
(19) Hartgerink, J. D.; Beniash, E.; Stupp, S. I. *Proc. Natl. A* **2002**, *99*, 5133−5138.
(20) Sugihara, S.; Kanakoa, S.; Aoshima, S. *J. Polym. Sci. Part A: Polym. Chem.* **2004**, *42*, 2601−2611.
(21) Hawker, C. J.; Bosman, A. W.; Harth, E. *Chem. Rev.* **2001**, *101*, 3661−3688.
(22) Lacroix-Desmazes, P.; Andre, P.; Desimone, J. M.; Ruzette, A.-V.; Boutevin, B. *J. Polym. Sci. Part A: Polym. Chem.* **2004**, *42*, 3537−3552.
(23) Matyjaszewski, K.; Xia, J. *Chem. Rev.* **2001**, *101*, 2921−2990.
(24) Barner-Kowollik, C.; Davis, T. P.; Heuts, J. P. A.; Stenzel, M. H.; Vana, P.; Whittaker, M. *J. Polym. Sci. Part A: Polym. Chem.* **2003**, *41*, 365−375.
(25) Rizzardo, E.; Chiefari, J.; Mayadunne, R. T. A.; Moad, G.; Thang, S. H. In *Controlled/Living Radical Polymerization. Progress in ATRP, NMP, and RAFT*; Matyjaszewski, K., Ed.; American Chemical Society: Washington DC, 2000; Vol. 768, pp 278−296.
(26) Donovan, M. S.; Lowe, A. B.; Sanford, T. A.; McCormack, C. L. *J. Polym. Sci. Part A: Polym. Chem.* **2003**, *41*, 1262−1281.
(27) Zhang, S.; Qing, J.; Xiong, C.; Peng, Y. *J. Polym. Sci. Part A: Polym. Chem.* **2004**, *42*, 3527−3536.
(28) Angot, S.; Ayres, N.; Bon, S. A. F.; Haddleton, D. M. *Macromolecules* **2001**, *34*, 768−774.
(29) Becker, M. L.; Liu, J.; Wooley, K. L. *Chem. Commun.* **2003**, 180−181.
(30) Mei, Y.; Beers, K. L.; Byrd, H. C. M.; VanderHart, D. L.; Washburn, N. R. *J. Am. Chem. Soc.* **2004**, *126*, 3472−3476.
(31) Sanji, T.; Nakatsuka, Y.; Kitayama, F.; Sakurai, H. *Chem. Commun.* **1999**, 2201−2202.
(32) Sanji, T.; Nakatsuka, Y.; Ohnishi, S.; Sakurai, H. *Macromolecules* **2000**, *33*, 8524−8526.
(33) Henselwood, F.; Liu, G. *Macromolecules* **1997**, *30*, 488.
(34) Bütün, V.; Billingham, N. C.; Armes, S. P. *J. Am. Chem. Soc.* **1998**, *120*, 12135.
(35) Thurmond, K. B., II.; Kowalewski, T.; Wooley, K. L. *J. Am. Chem. Soc.* **1996**, *118*, 7239−7240.
(36) Pan, D.; Turner, J. L.; Wooley, K. L. *Chem. Commun.* **2003**, 2400−2401.
(37) Huang, H.; Kowalewski, T.; Wooley, K. L. *J. Polym. Sci. Part A: Polym. Chem.* **2003**, *41*, 1659−1668.
(38) Thurmond, K. B., II.; Remsen, E. E.; Kowalewski, T.; Wooley, K. L. *Nucleic Acids Res.* **1999**, *27*, 2966−2971.
(39) Liu, J.; Zhang, Q.; Remsen, E. E.; Wooley, K. L. *Biomacromolecules* **2001**, *2*, 362−368.
(40) Becker, M. L.; Bailey, L. O.; Wooley, K. L. *Bioconjugate Chem.* **2004**, *15* (4), 710−717.
(41) Becker, M. L.; Remsen, E. E.; Pan, D.; Wooley, K. L. *Bioconjugate Chem.* **2004**, *15* (4), 699−709.
(42) Schibli, D. J.; Hwang, P. M.; Vogel, H. J. *Biochemistry* **1999**, *38*, 16749−16755.
(43) Remsen, E. E.; Thurmond, K. B., II.; Wooley, K. L. *Macromolecules* **1999**, *32*, 3685−3689.
(44) Lawer, C.; Pai, S.; Watabe, M.; Mashimo, T.; Eagleton, L.; Watabe, K. *FEBS Lett.* **1996**, *390*, 95−98.
(45) Zanetti, M.; Gennaro, R.; Romeo, D. *FEBS Lett.* **1995**, *374*, 1−5.
(46) Panyutich, A.; Shi, J.; Boutz, P. L.; Zhao, C.; Ganz, T. *Infect. Immun.* **1997**, *65*, 978−985.
(47) Schibli, D. J.; Epand, R. F.; Vogel, H. J.; Epand, R. M. *Biochem. Cell. Biol.* **2002**, *80*, 667−677.
(48) Yang, S.-T.; Shin, S. Y.; Lee, C. W.; Kim, Y.-C.; Hahm, K.-S.; Kim, J. I. *FEBS Lett.* **2003**, *540*, 229−233.
(49) Benoit, D.; Chaplinski, V.; Braslau, R.; Hawker, C. J. *J. Am. Chem. Soc.* **1999**, *121*, 3904−3920.
(50) Dao, J.; Benoit, D.; Hawker, C. J. *J. Polym. Sci., Part A: Polym. Chem.* **1998**, *36*, 2161−2167.
(51) Ma, Q.; Wooley, K. L. *J. Polym. Sci., Part A: Polym. Chem.* **2000**, *38*, 4805−4820.
(52) Becker, M. L.; Remsen, E. E.; Wooley, K. L. *J. Polym. Sci. Part A: Polym. Chem.* **2001**, *39*, 4215.
(53) Hansen, M. B.; Nielsen, S. E.; Berg, K. *Immunol. Methods* **1989**, *119*, 203-210.
(54) Becker, M. L.; Wooley, K. L. unpublished results.

BM049551Y